Electronic Supplementary Material (ESI) for ChemComm.

Supporting Information

Materials and Methods

References

Materials and Methods

Bioinformatics analysis of putative rG4s in mature miRNAs

We performed a computational survey of all characterized miRNAs from different organisms, to evaluate the potential of mature miRNA sequences to fold into competing rG4 structures, and to estimate the frequency of such cases. All sequences were obtained from miRBase[1] version 22. Putative rG4 sequences were estimated both *via* regular expression search to conform general rG4 favoring architecture[2], and *via* the calculation of G4NN probability scores based on the published artificial neural network (ANN)-based model for RNA G4 formation[3]. The latter model was created specifically for RNA G-quadruplex sequences, hence capturing their stability differences from more computationally-studied DNA G-quadruplexes[4, 5], and is permissive to non-canonical G4 sequences with bulges or shorter G-tracts. Given the short span of mature RNA sequences (~22 nucleotides), we used a more permissive regular expression ($G_{2+}N_{1-12}G_{2+}N_{1-12}G_{2+}N_{1-12}G_{2+}$, denoted elsewhere as G2L12), allowing for the individual G-tracts to be at least 2-nucleotides, and the loop sizes to be no longer than 12 nucleotides[5] in length. This approach identified 886 mature miRNA sequences with putative rG4s in miRBase version 22 (Table S1), of which 191 are in *Homo sapiens* (7 % of all human mature miRNAs). The ANN-based model identified 5160 mature miRNAs with putative rG4s (Table S1, G4NN > 0.5), of which 478 are in *Homo sapiens* (18 % of all human mature miRNAs). The overlap between the two approaches (G2L12 motif and ANN-based model G4NN > 0.5) results in 166 human mature miRNAs with high-confidence putative rG4s, also conforming an easily understood sequence motif for further analyses and mutagenesis. Out of those 166 miRNAs (6% of all human mature miRNAs), we next picked 4 (miR-149, miR-197, miR-432 and miR-765) to perform further experiments. The selection was done based on their biological relevance, belonging to the high-confidence 166 sequences, their general conservation pattern across species (Table S2), and representation of various G4NN probabilities in the rG4-positive 0.5 to 1.0 range[3] (0.997, 0.665, 0.549 and 0.717 for miR-149, miR-197, miR-432 and miR-765 sequences correspondingly). Interestingly, the sequences with highest and lowest G4NN probabilities (still within the realm of producing stable rG4s) had highest (71 ^{o}C for miR-149) and lowest (40 ^{o}C for miR-432) rG4 melting temperatures (Tms) correspondingly, as assessed *via* UV melting studies (Fig. S5 and S7).

Oligonucleotides and ligands

RNA oligonucleotides investigated in this study were purchased commercially (TechDragon). Sequences are listed in Table S3. The 5'FAM-miRNAs were further size fractioned on a 7M urea, 15% denaturing polyacrylamide gel and visualized under brief UV shadowing. The gel slices that contained the desired RNA band were crushed and soaked overnight at 4°C in 10 mM Tris-HCl (pH 7.4), 1 mM EDTA and 800 mM LiCl (1× TEL-800 buffer) in dark with constant agitation[6]. The gel mixture was then filtered through Corning® Costar® Spin-X® centrifuge tube filter (0.22 μm) and the RNA was purified using RNA Clean & Concentrator™-5 (Zymo Research)[7]. All RNAs were dissolved in nuclease-free water, quantified by NanoDrop and stored at -20°C.

N-methyl-mesoporphyrin IX (NMM) and Thioflavin T (ThT) were purchased from Frontier scientific and Solarbio Life Sciences respectively.

Circular dichroism (CD) spectroscopy

CD spectroscopy was performed using Jasco CD J810 spectropolarimeter and a 1-cm path length quartz cuvette with a reaction volume of 2 ml[6]. 5 μM RNAs were prepared in 10 mM LiCac (pH 7.0) and 150 mM KCl or LiCl. Before detection, RNAs were denatued at 95°C for 5 mins and cooled to room temperature for 10 min for renaturation. Spectra were acquired every 1 nm from 220 to 310 nm at 25°C for wildtype and mutant miRNAs. Data were smoothed over 5 nm.

Thermal melting monitored by UV spectroscopy

Thermal melting monitored by UV spectroscopy was performed using Cary 100 UV-Vis spectrophotometer and a 1-cm path length quartz cuvette with a reaction volume of 2 ml[7]. Samples were prepared and renatured as per CD experiment above. Data were collected over 0.2°C while heating over the temperature range 20-95°C. The unfolding transitions were monitored at 295 nm for wildtype and mutant miRNAs to look for the inverse melting GQS signature, unless otherwise stated. For concentration-dependent UV melting experiments, the RNA concentration between 2.5-10 μM was used. For UV melting experiments in the presence of seed match oligonucleotide or NMM, the seed match or NMM was added after the 10 min renaturation step as described in the CD experiment above. Data were smoothed over 5 nm.

Fluorescence spectroscopy

Fluorescence spectroscopy was performed using HORIBA FluoroMax-4 and a 1-cm path length quartz cuvette with a reaction volume of 100 µl. 2 µM RNAs were prepared in 10 mM LiCac (pH 7.0) and 150 mM KCl or LiCl. Before detection, RNAs were denatued at 95°C for 3 mins and cooled to room temperature for 10 min for renaturation. 2 µl of 100 µM NMM or 100 µM ThT (final conc. 2 µM) were added separately. The sample was excited at 393 nm (for NMM) and 425 nm (for ThT). The emission spectrum was collected from 580-700 nm for NMM, and 440-700 nm for ThT respectively. Spectra were acquired every 2 nm at 25°C for wildtype and mutant miRNAs. The entrance and exit slits were 5 and 2 nm, respectively.

In-line probing (ILP) and RNA sequencing ladders

Each ILP reaction was performed in 10 µl reaction. First, 1 µl of 5'FAM-labelled RNA (4 µM) and 4 µl of nuclease-free water were mixed. The RNA was heated at 95°C for 30 sec and cooled to room temperature for 5 min for renaturation. Then, 5 µl of 2× ILP buffer containing 300 mM LiCl or KCl, 10 mM $MgCl_2$ and 50 mM Tris/HCl (pH 8.3) was added. The reaction mixture was incubated at 37°C for 40 h. In order to test the binding of seed sequence on G-qudraplex miRNAs, nuclease-free water was replaced by 4 µl of 1 µM or 10 µM seed sequence

A denaturing RNase T1 ladder was produced using 1 µl of 5'FAM-labelled RNA (4 µM) and 8 µl of 1.25× reaction buffer containing 10 M urea, 1 M sodium acetate (pH 5.2), 0.1 M EDTA. The RNA was heated at 95°C for 30 sec and cooled to 37°C for 15 min for renaturation. 1 µl of 10× RNase T1 (5 units/µl) was added. The reaction mixture was incubated at 37°C for 15 min and cool down to room temperature for 3 min. A hydrolysis ladder was produced by incubating 1 µl of 5'FAM-labelled RNA (4 µM) and 9 µl of 1× reaction buffer containing 20 mM NaOH at 95°C for 1 min and cool down to room temperature for 3 min.

All the reactions were quenched by mixing with an equal volume of 2× stop solution, which contains 94% deionized formamide, 20 mM Tris/HCl (pH 7.5), 20 mM EDTA and organe G for tracking. After heating up at 95°C, 2 µl of all reactions were loaded on a 8 M urea, 8% denaturing polyacrylamide gel and visualized by Fujifilm FLA-9000, and data were quantified by Image J.

Transfection and luciferase reporter assay

The wildtype and mutant miRNA response elements (MREs) of miR-149, miR-197, miR-432, and miR-765 were annealed from complementary oligonucleotides (BGI, China) and ligated to the Firefly/Renilla luciferase reporter vector, psiCHECK-2 (Promega, USA), between NotI and XhoI restriction enzyme sites at the 3' end of the Renilla luciferase gene. HEK-293T cells were seeded in 96-well black-wall optical plates (Perkin Elmer) at the density of 50,000 cells/well. The HEK-293T cells are originally from American Type Culture Collection (ATCC, USA). We have validated the identity of the cells using a 16-loci multiplex short tandem repeat analysis according to ATCC standards, provided by an authentication service from Guangzhou IGE Biotechnology (China). In each well, the cells were transfected with 12.5 nM miRNA mimics or scrambled control mimics (Shanghai GenePharma, China) and 10 ng luciferase reporter plasmid using Lipofectamine® 2000 according to the manufacturer's protocol (Thermo Fisher Scientific, USA). After 5 and 24 hours, the medium was replaced with fresh medium containing 80 μM NMM (Frontier scientific) or 80 μM DMSO (Sigma Aldrich). The cells were harvested 48 hours after transfection for the luciferase reporter assay using the Dual Luciferase Reporter Assay System (Promega, USA) according to the manufacturer's manual. Firefly and Renilla luciferase activities were determined using the Synergy H1 microplate reader (Biotek, USA). Renilla luciferase activity was normalized to Firefly luciferase activity (Firefly luciferase is constitutively expressed by psi-Check2 as an internal control) and presented as the average of three transfection repeats.

Table S1. Putative rG4s in mature miRNAs in human and other organisms. See the additional Supporting Information Table S1 brought in an Excel format. Data is also available on http://github.com/aleksahak/miRNA-G4s.

Table S2. miRBase accession of selected mammalian-conserved miRNA candidates (miR-149, miR-197, miR-432, miR-765) that contains putative rG4.

miRNA	Mammalian species	miRBase accession ID
miR-149	*Homo sapiens*	MI0000478
	Bos Taurus	MI0021115
	Macaca mulatta	MI0007640
	Cavia porcellus	MI0038658
	Dasypus novemcinctus	MI0038999
	Mus musculus	MI0000171
	Cricetulus griseus	MI0020411
miR-197	*Homo sapiens*	MI0000239
	Cavia porcellus	MI0038688
	Dasypus novemcinctus	MI0039031
	Macaca mulatta	MI0007661
	Oryctolagus cuniculus	MI0039337
miR-432	*Homo sapiens*	MI0003133
	Ovis aries	MI0001522
	Macaca mulatta	MI0007744
	Pan troglodytes	MI0008667
	Bos taurus	MI0009831
	Canis familiaris	MI0010403
	Equus caballus	MI0012901
	Pongo pygmaeus	MI0014944
	Capra hircus	MI0030792
	Cavia porcellus	MI0038774
	Dasypus novemcinctus	MI0039109
	Oryctolagus cuniculus	MI0039405
	Callithrix jacchus	MI0040062
miR-765	*Homo sapiens*	MI0005116
	Pan troglodytes	MI0008859
	Pongo pygmaeus	MI0015145
	Macaca mulatta	MI0007910

miRNAs were queried in miRBase[1] version 22 (http://www.mirbase.org).

Table S3. RNA sequences used in this study.

Name	Modification	Sequence (5'-3')
miR-149	/	AGGGAGGGACGGGGGCUGUGC
miR-197	/	CGGGUAGAGAGGGCAGUGGGAGG
miR-432	/	UCUUGGAGUAGGUCAUUGGGUGG
miR-765	/	UGGAGGAGAAGGAAGGUGAUG
miR-149_mut	/	AGGGAAAAACAAAAACUGUGC
miR-197_mut	/	CGGGUAGAGAAAACAGUAAAAGG
miR-432_mut	/	UCUUGGAGUAAAUCAUUAAAUGG
miR-765_mut	/	UGGAAAAGAAAAAAGGUGAUG
miR-149_seed match	/	CCCUCCC
miR-197_seed match	/	UCUACCC
miR-432_seed match	/	CUCCAAG
miR-765_seed match	/	CUCCUCC
5'FAM_miR-149	5'FAM-	AGGGAGGGACGGGGGCUGUGC
5'FAM_miR-197	5'FAM-	CGGGUAGAGAGGGCAGUGGGAGG
5'FAM_miR-432	5'FAM-	UCUUGGAGUAGGUCAUUGGGUGG
5'FAM_miR-765	5'FAM-	UGGAGGAGAAGGAAGGUGAUG
Scrambled miRNA mimic	/	UUGUACUACACAAAAGUACUG

The seed regions of the 5'FAM labelled miRNAs are shown in green. The seed match sequences (blue) are reverse complement to the miRNA seed region. The mutant miRNAs are designed by using As (underlined) to substitute some Gs with potential to participate in an rG4.

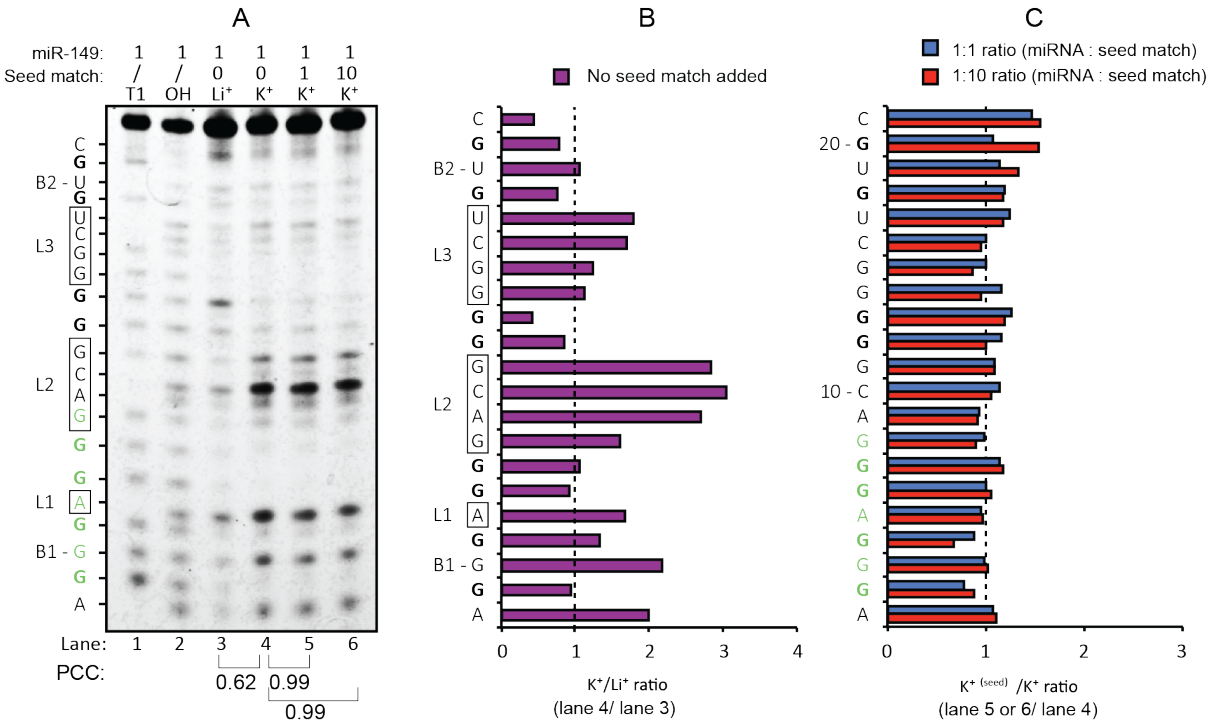

Figure S1. In-line probing (ILP) results and analyses of miR-149. MiR-149, which contains a putative rG4, was subjected to ILP under 150mM Li^+-containing and 150mM K^+-containing conditions at physiological relevant temperature (37°C). **A)** RNA was size-fractionated on denaturing polyacrylamide gel after the ILP reaction. Lane 1 shows the hydrolysis ladder (every nucleotides), lane 2 shows the RNase T1 ladder (Gs only). Lanes 3-6 show ILP cleavage under Li^+, K^+, K^+ plus one equivalent concentration of seed match sequence in mRNA added, and K^+ plus ten equivalent of seed match sequence in mRNA. The Gs in the G-quartets are shown in bold, the bulges in the G-quartets are labelled as "B1" and "B2" and the three loops regions are boxed and labeled as "L1", "L2" and "L3". The miRNA seed region is shown in green. The in-line cleavage pattern under K^+ condition suggested the occurrence of two bulges (B1 and B2) at the G-quadruplex cores of both end. The occurrence of bulges in G-quadruplex structure is not uncommon and has been reported[8]. The Pearson correlation coefficient (PCC) reports the correlation of band intensities between conditions, with PCC of 1 being perfect positive correlation. **B)** K^+/Li^+ ratio report the nucleotides that are more exposed (>1) or more protected (<1) by changing from Li^+ to K^+ condition. Most nucleotides on the loops of rG4 (L1, L2, L3) are more exposed, whereas most Gs involved in rG4 (bolded Gs) are protected. **C)** $K^{+\,(seed)}/K^+$ ratio report the nucleotides that are more exposed (>1) or more protected (<1) by addition of seed match sequence in mRNA (at one or ten equivalent). miRNA seed region (nucleotides 2-8, green) that interact with the seed match sequence (7 nucleotides) are not protected, suggesting the rG4 structure were not affected.

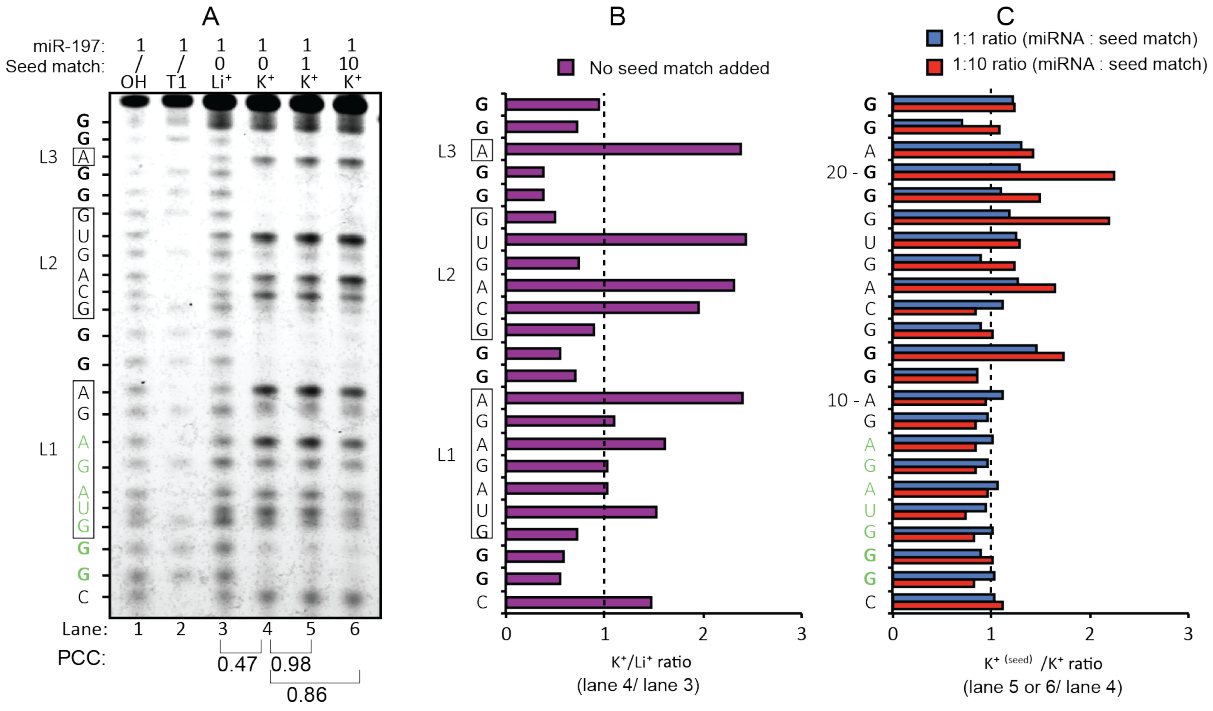

Figure S2. In-line probing (ILP) results and analyses of miR-197. MiR-197, which contains a putative rG4, was subjected to ILP under 150mM Li^+-containing and 150mM K^+-containing conditions at physiological relevant temperature (37°C). **A)** RNA was size-fractionated on denaturing polyacrylamide gel after the ILP reaction. Lane 1 shows the hydrolysis ladder (every nucleotides), lane 2 shows the RNase T1 ladder (Gs only). Lanes 3-6 show ILP cleavage under Li^+, K^+, K^+ plus one equivalent concentration of seed match sequence in mRNA added, and K^+ plus ten equivalent of seed match sequence in mRNA. The Gs in the G-quartets are shown in bold, and the three loops regions are boxed and labelled as "L1", "L2" and "L3". The miRNA seed region is shown in green. The in-line cleavage pattern under K^+ condition suggested the occurrence of two G-quartets structure with long loops (>4 nt loop). The occurrence of long loops in G-quadruplex structure with two G-quartets is not uncommon and has been reported[9]. The Pearson correlation coefficient (PCC) reports the correlation of band intensities between conditions, with PCC of 1 being perfect positive correlation. **B)** K^+/Li^+ ratio report the nucleotides that are more exposed (>1) or more protected (<1) by changing from Li^+ to K^+ condition. Most nucleotides on the loops of rG4 (L1, L2, L3) are more exposed, whereas most Gs involved in rG4 (bolded Gs) are protected. **C)** $K^{+\,(seed)}/K^+$ ratio report the nucleotides that are more exposed (>1) or more protected (<1) by addition of seed match sequence in mRNA (at one or ten equivalent). miRNA seed region (nucleotides 2-8, green) that interact with the seed match sequence (7 nucleotides) are not protected, suggesting the rG4 structure were not affected.

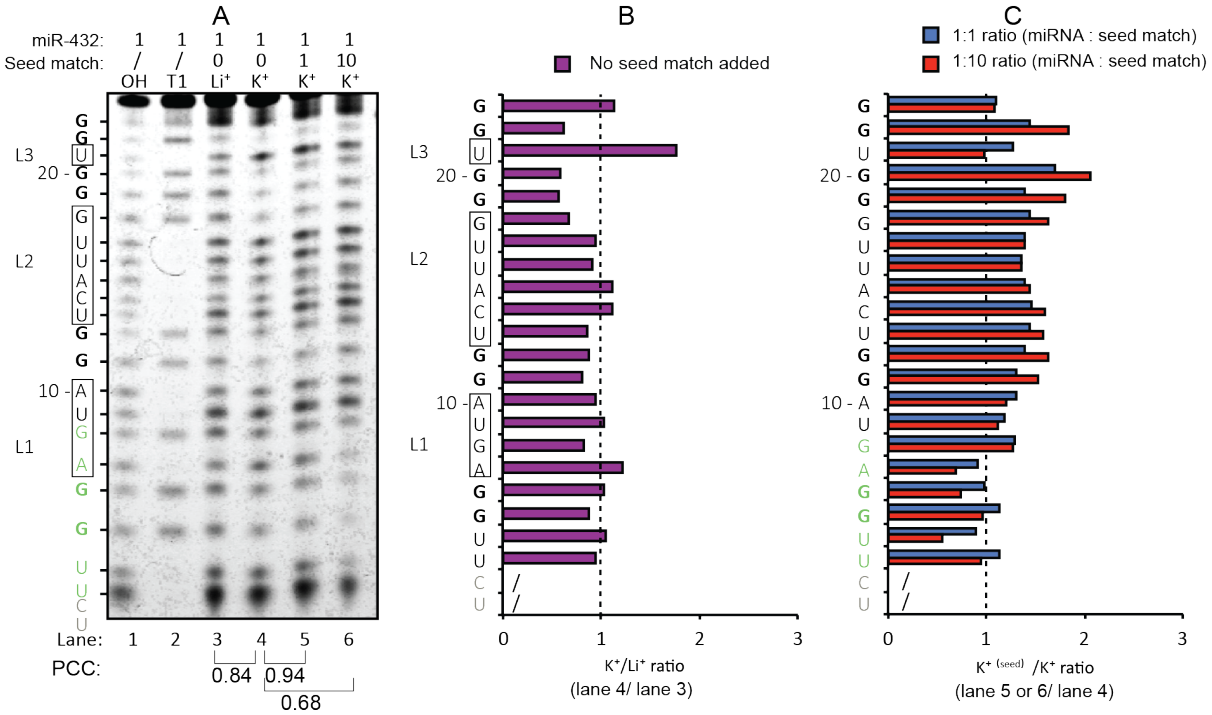

Figure S3. In-line probing (ILP) results and analyses of miR-432. MiR-432, which contains a putative rG4, was subjected to ILP under 150mM Li^+-containing and 150mM K^+-containing conditions at physiological relevant temperature (37°C). **A)** RNA was size-fractionated on denaturing polyacrylamide gel after the ILP reaction. Lane 1 shows the hydrolysis ladder (every nucleotides), lane 2 shows the RNase T1 ladder (Gs only). Lanes 3-6 show ILP cleavage under Li^+, K^+, K^+ plus one equivalent concentration of seed match sequence in mRNA added, and K^+ plus ten equivalent of seed match sequence in mRNA. The Gs in the G-quartets are shown in bold, and the three loops regions are boxed and labelled as "L1", "L2" and "L3". The miRNA seed region is shown in green. The in-line cleavage pattern under K^+ condition suggested the occurrence of two G-quartets structure with long loops (>4nt loop), which has been recently reported[9]. The Pearson correlation coefficient (PCC) reports the correlation of band intensities between conditions, with PCC of 1 being perfect positive correlation. The bands at the 5' end of the miRNA were compressed and cannot be resolved (U and C nt, grey). **B)** K^+/Li^+ ratio report the nucleotides that are more exposed (>1) or more protected (<1) by changing from Li^+ to K^+ condition. As the Tm of miR-432 is 40°C (see Fig. S7), the rG4 pattern is not as obvious as other miRNA cases. Some nucleotides on the loops of rG4 are more exposed, whereas most Gs involved in rG4 are protected. **C)** $K^{+\,(seed)}/K^+$ ratio report the nucleotides that are more exposed (>1) or more protected (<1) by addition of seed match sequence (at one or ten equivalent). miRNA seed region that interact with the seed match are protected at ten equivalent (see gel in A).

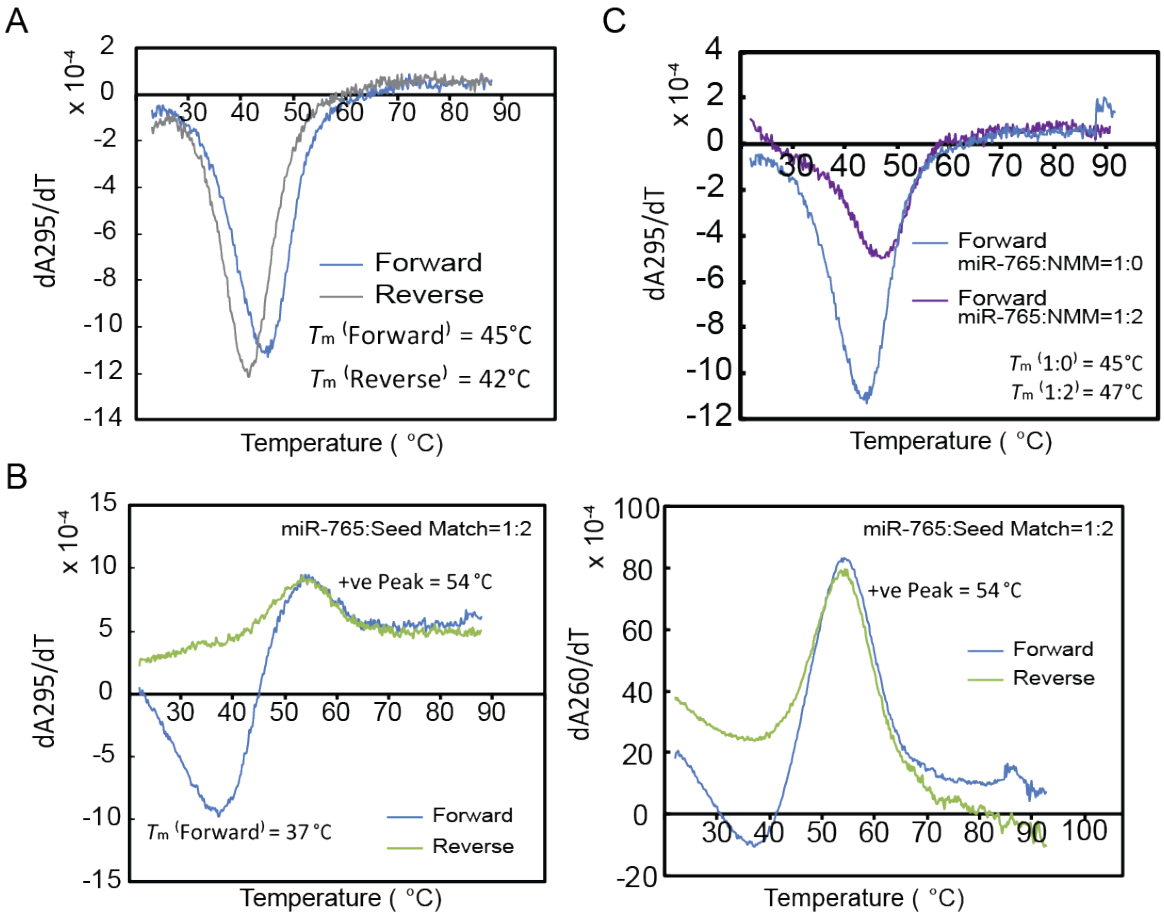

Figure S4. UV melting data and analysis of rG4 in miR-765. A) Forward and reverse UV melting of miR-765 under K^+ condition. The melting temperature (Tm) between forward (melting) and reverse (annealing) curve had a slight hysteresis of 3°C, which is not uncommon for G-quadruplex melting experiments[10-12]. This slight hysteresis is due to the minor difference between the melting and annealing kinetics of rG4, and 3°C difference between melting and annealing curve is small[10, 11] and the G4 folding/unfolding is still regarded as thermodynamic equilibrium[10]. **B)** UV melting of miR-765 in the presence of seed match oligonucleotide. miR-765 and its corresponding seed match is at a ratio of 1:2. **Left:** The addition of the seed match decreases the hypochromic melting transition of miR-765 in the melting (forward) curve monitored at 295 nm, from 45°C to 37°C (compare blue forward curve in A and B). In addition, the annealing (reverse) curve shows an appearance of a new melting transition at 54°C, which is likely the competitive structure as suggested by our in-line probing results (Figure 2). **Right:** Same experiment was also observed at 260 nm, which support the RNA duplex formed between miR-765 plus seed match. This competitive structure is more thermostable than rG4 in miR-765 (54°C vs 45°C). **C)** UV melting of miR-765 in the presence of NMM. miR-765 and NMM is at a ratio of 1:2 and forward melting curve were shown. NMM stabilizes the rG4 in the miR-765 *in vitro*, from 45°C to 47°C.

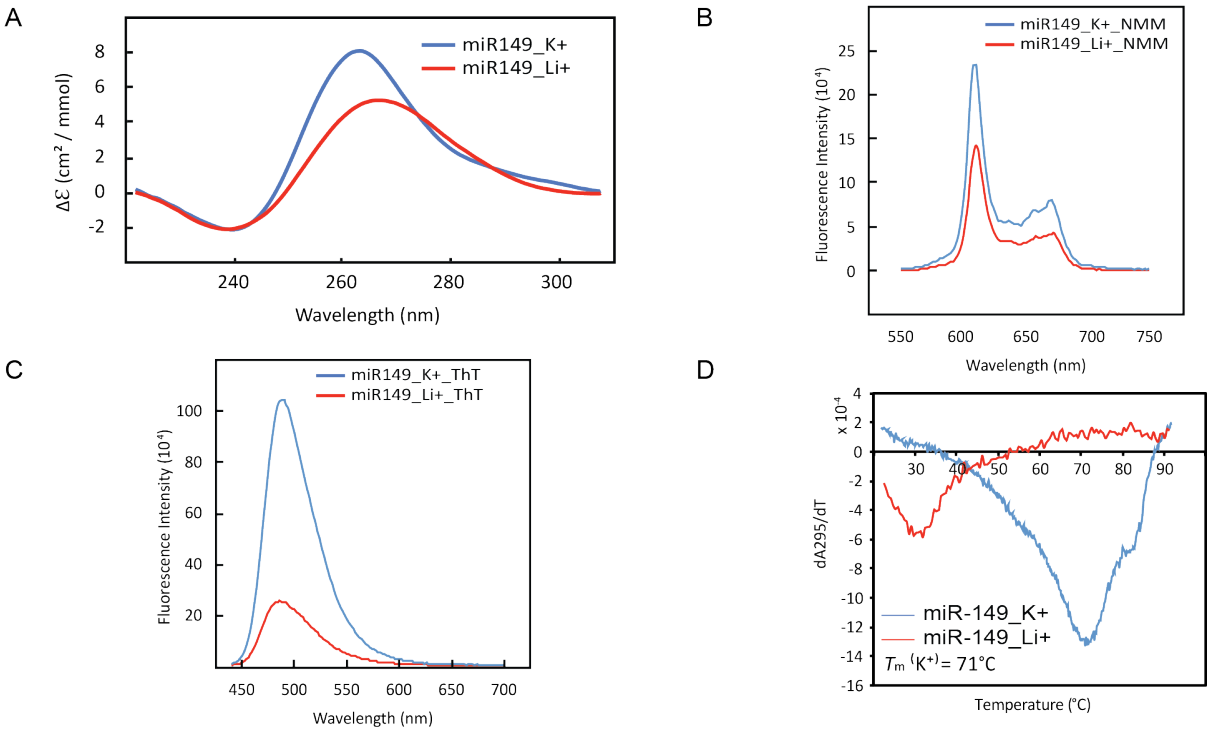

Figure S5. Biophysical characterization of rG4 in miR-149. A) CD spectrum shows a distinct signature under K^+ but not in Li^+ conditions, suggesting the formation of a parallel topology rG4 structure. **B-C)** Fluorescence spectra show augmented fluorescence under K^+ as compared to Li^+ conditions, indicating the presence of rG4 for G4 ligands (B. NMM and C. ThT) recognition and fluorescence enhancement. **D)** UV melting shows increased rG4 thermostability from 30°C (Li^+ condition) to 71°C (K^+ condition), suggesting the rG4 is thermostable at physiological temperature under K^+ condition.

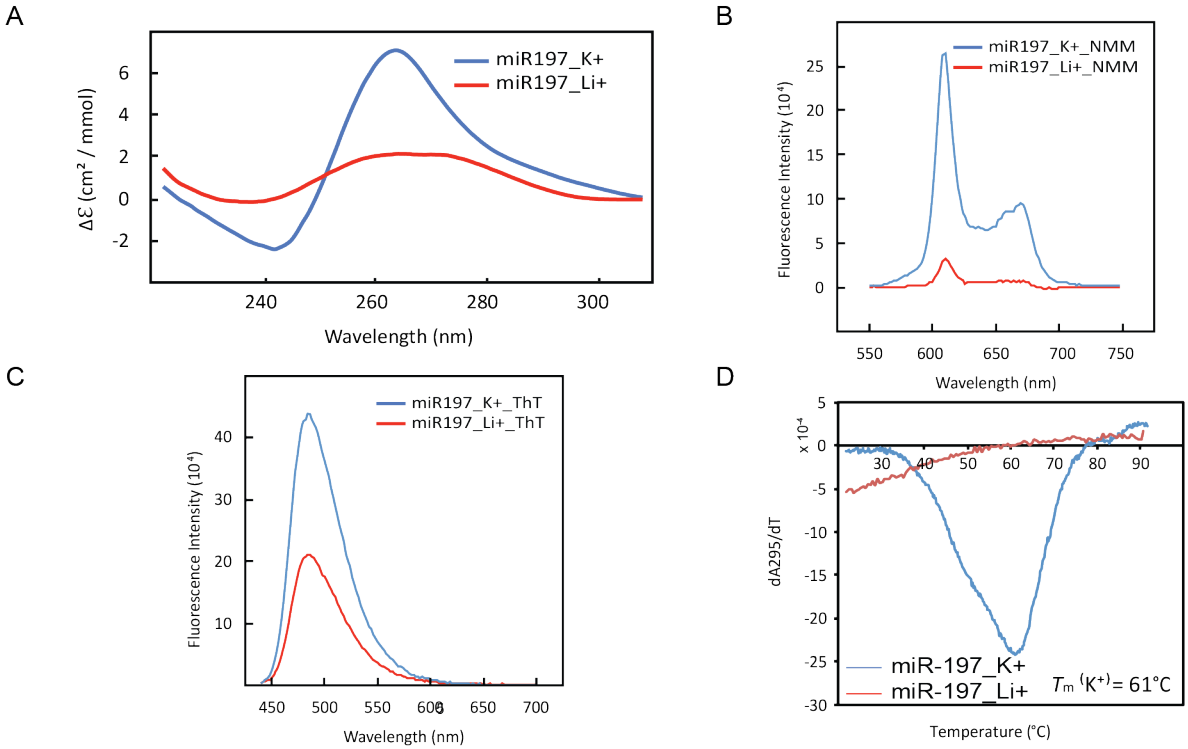

Figure S6. Biophysical characterization of rG4 in miR-197. A) CD spectrum shows a distinct signature under K^+ but not in Li^+ conditions, suggesting the formation of a parallel topology rG4 structure. **B-C)** Fluorescence spectra show augmented fluorescence under K^+ as compared to Li^+ conditions, indicating the presence of rG4 for G4 ligands (B. NMM and C. ThT) recognition and fluorescence enhancement. **D)** UV melting shows characteristic hypochromic shift at 295 nm with rG4 thermostability at 61°C (K^+ condition), suggesting the rG4 is thermostable at physiological temperature under K^+ condition.

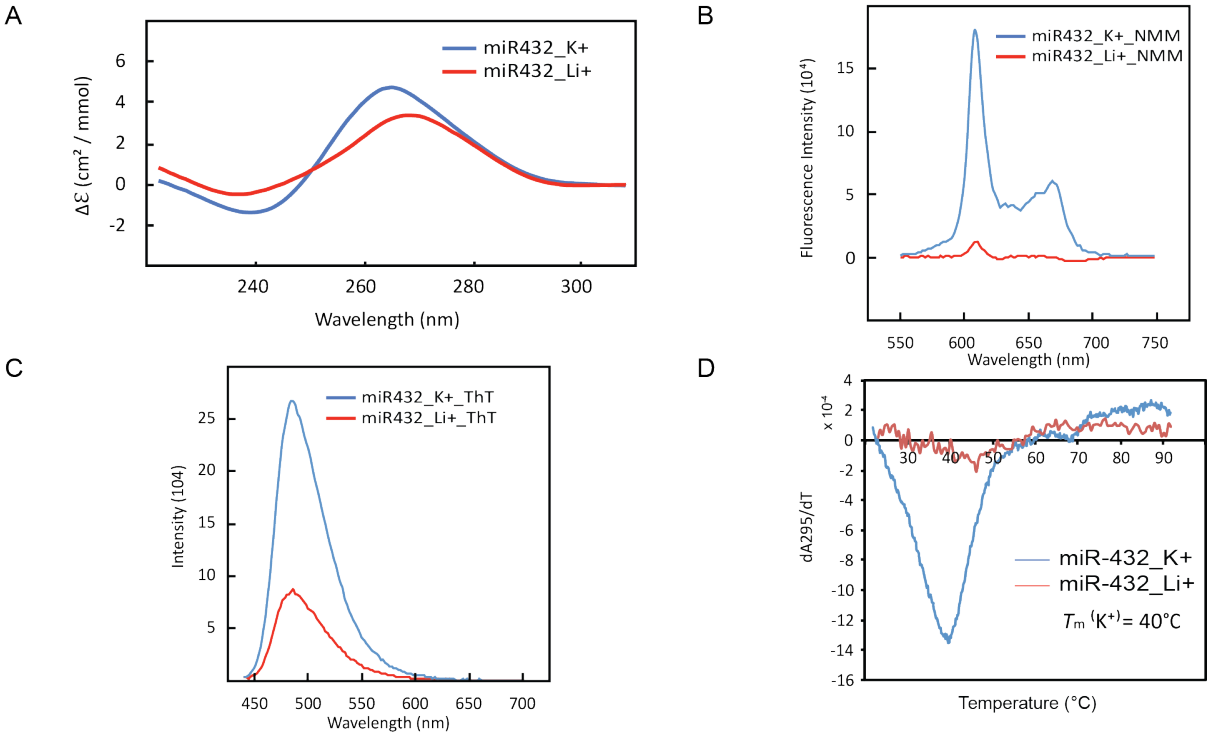

Figure S7. Biophysical characterization of rG4 in miR-432. A) CD spectrum shows a distinct signature under K^+ but not in Li^+ conditions, suggesting the formation of a parallel topology rG4 structure. **B-C)** Fluorescence spectra show augmented fluorescence under K^+ as compared to Li^+ conditions, indicating the presence of rG4 for G4 ligands (B. NMM and C. ThT) recognition and fluorescence enhancement. **D)** UV melting shows characteristic hypochromic shift at 295 nm with rG4 thermostability at 40°C (K^+ condition), suggesting the rG4 is thermostable at physiological temperature under K^+ condition.

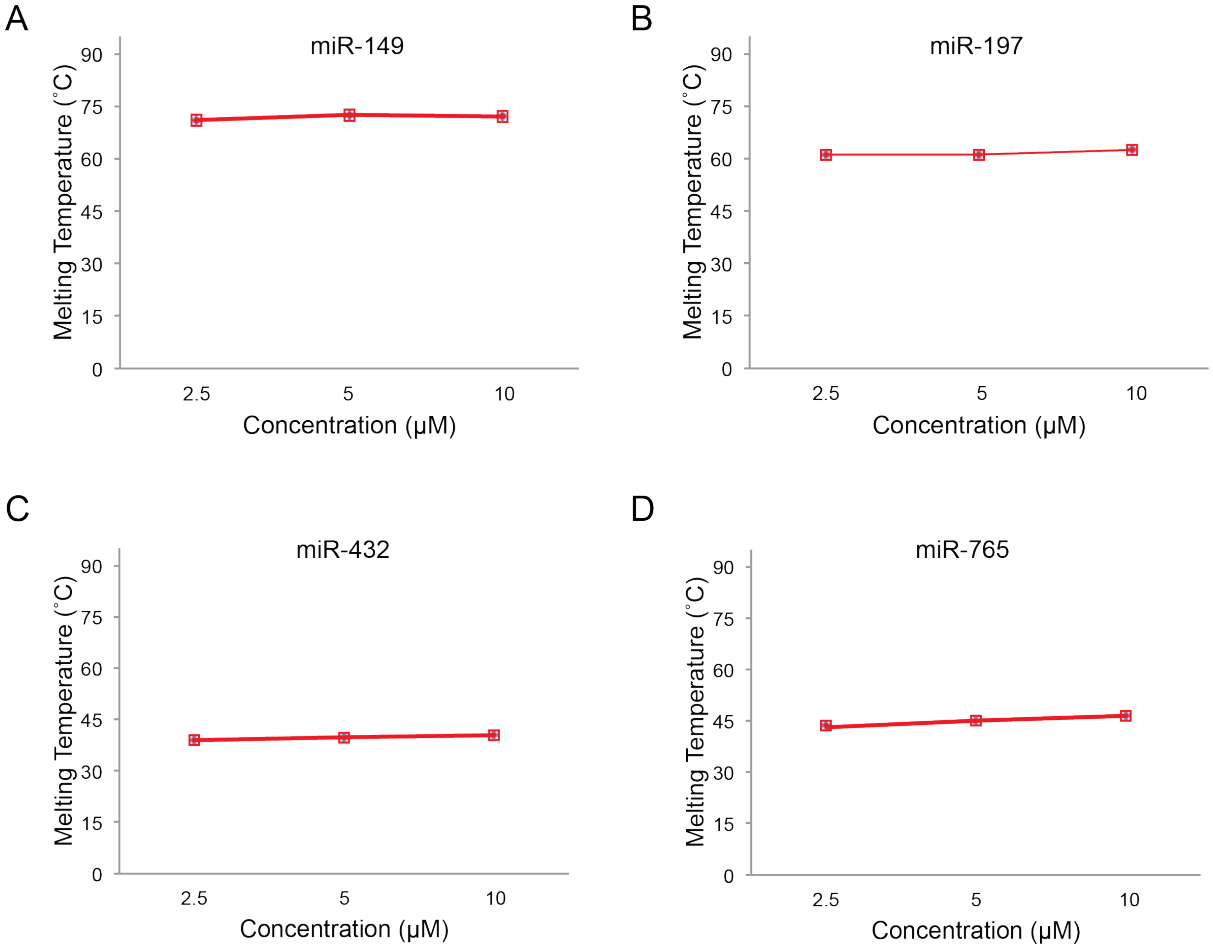

Figure S8. Concentration-dependent UV melting of **A)** miR-149, **B)** miR-197, **C)** miR-432, and **D)** miR-765. The melting temperature (Tm) of G-quadruplex of each miRNA is independent of the oligonucleotide concentration, suggesting that the UV signal observed is due to intramolecular rG4 folding.

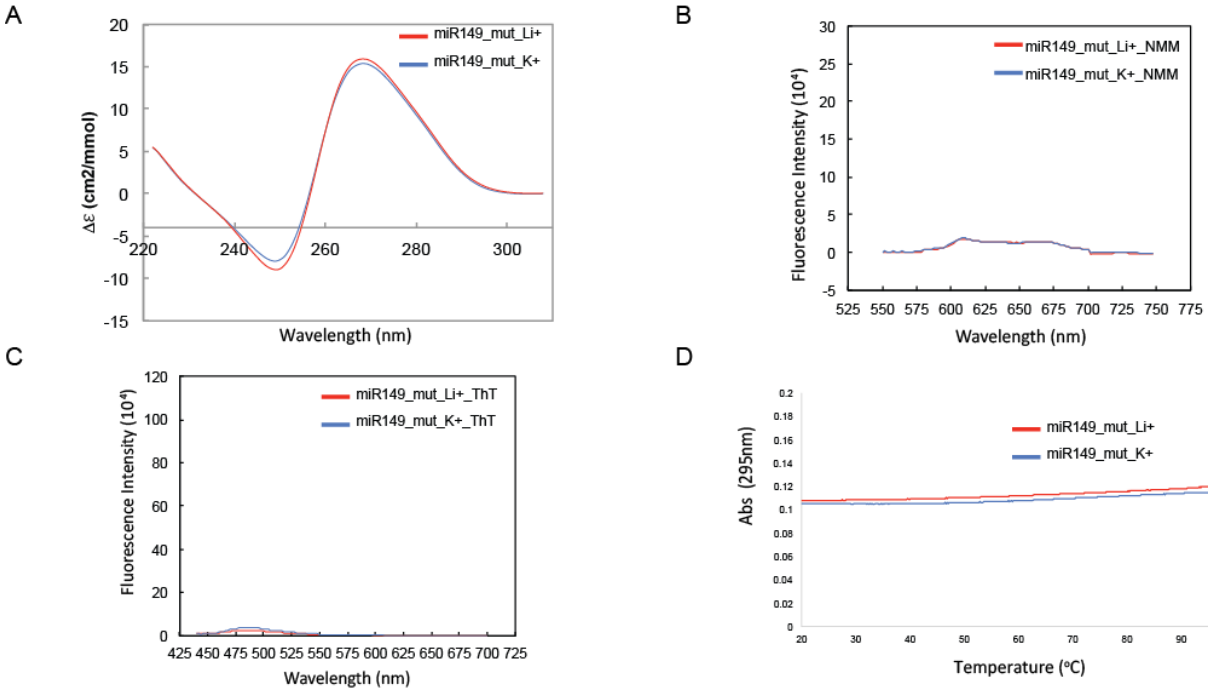

Figure S9. Biophysical characterization of rG4 in miR-149 mutant. A) CD spectrum shows almost no change in the profile under K^+ and Li^+ conditions. **B-C)** Fluorescence spectra show almost identical background fluorescence under K^+ and Li^+ conditions (compare with Fig. S5B-C). **D)** UV melting shows no hypochromic shift at 295 nm. The results of these 4 biophysical assays suggest that no rG4 is formed in the miR-149 mutant.

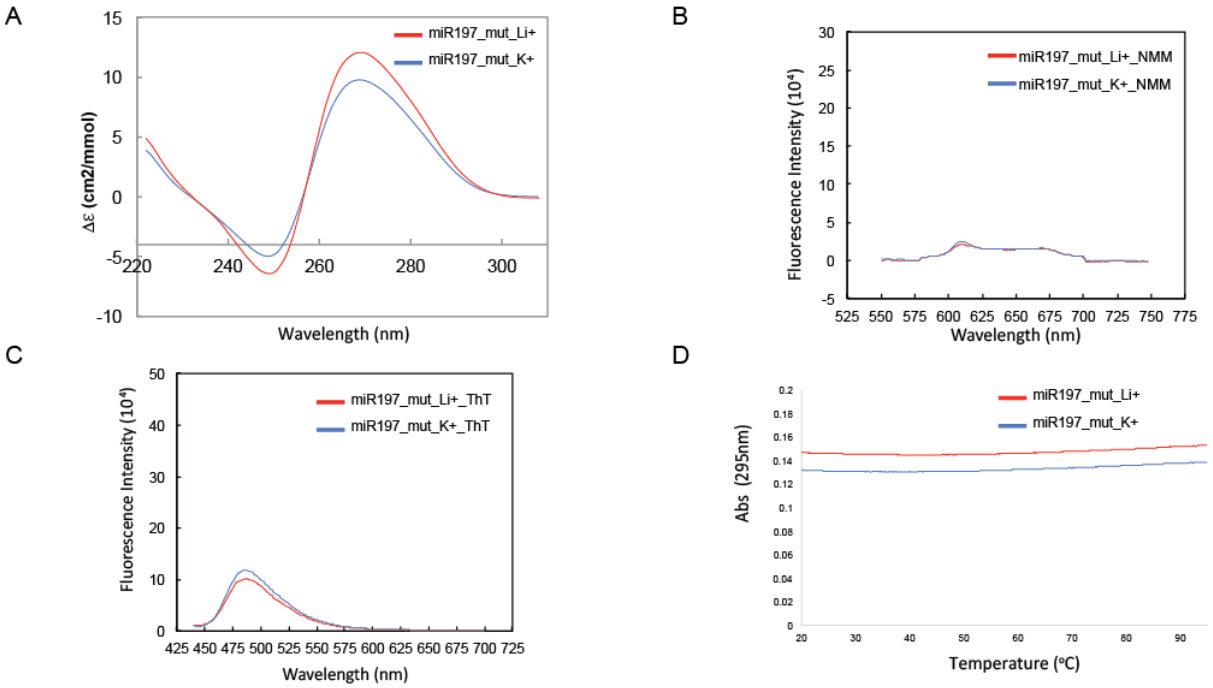

Figure S10. Biophysical characterization of rG4 in miR-197 mutant. A) CD spectrum shows almost no change in the profile under K^+ and Li^+ conditions. **B-C)** Fluorescence spectra show almost identical background fluorescence under K^+ and Li^+ conditions (compare with Fig. S6B-C). **D)** UV melting shows no hypochromic shift at 295 nm. The results of these 4 biophysical assays suggest that no rG4 is formed in the miR-197 mutant.

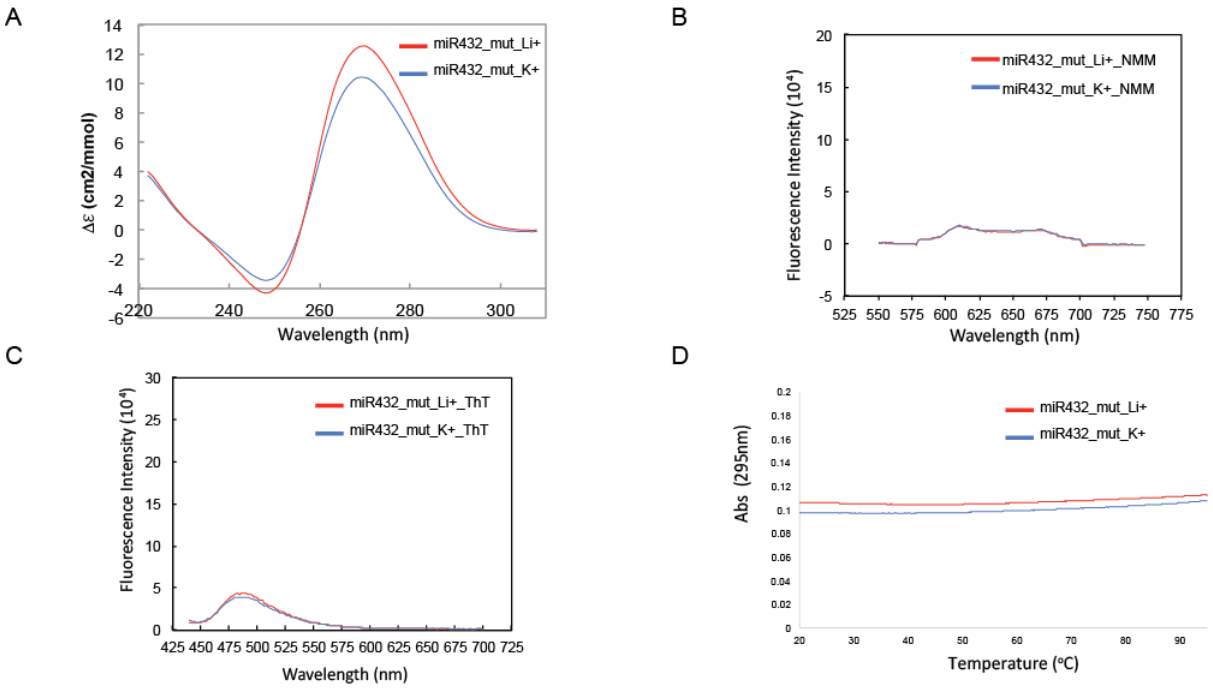

Figure S11. Biophysical characterization of rG4 in miR-432 mutant. A) CD spectrum shows almost no change in the profile under K^+ and Li^+ conditions. **B-C)** Fluorescence spectra show almost identical background fluorescence under K^+ and Li^+ conditions (compare with Fig. S7B-C). **D)** UV melting shows no hypochromic shift at 295 nm. The results of these 4 biophysical assays suggest that no rG4 is formed in the miR-432 mutant.

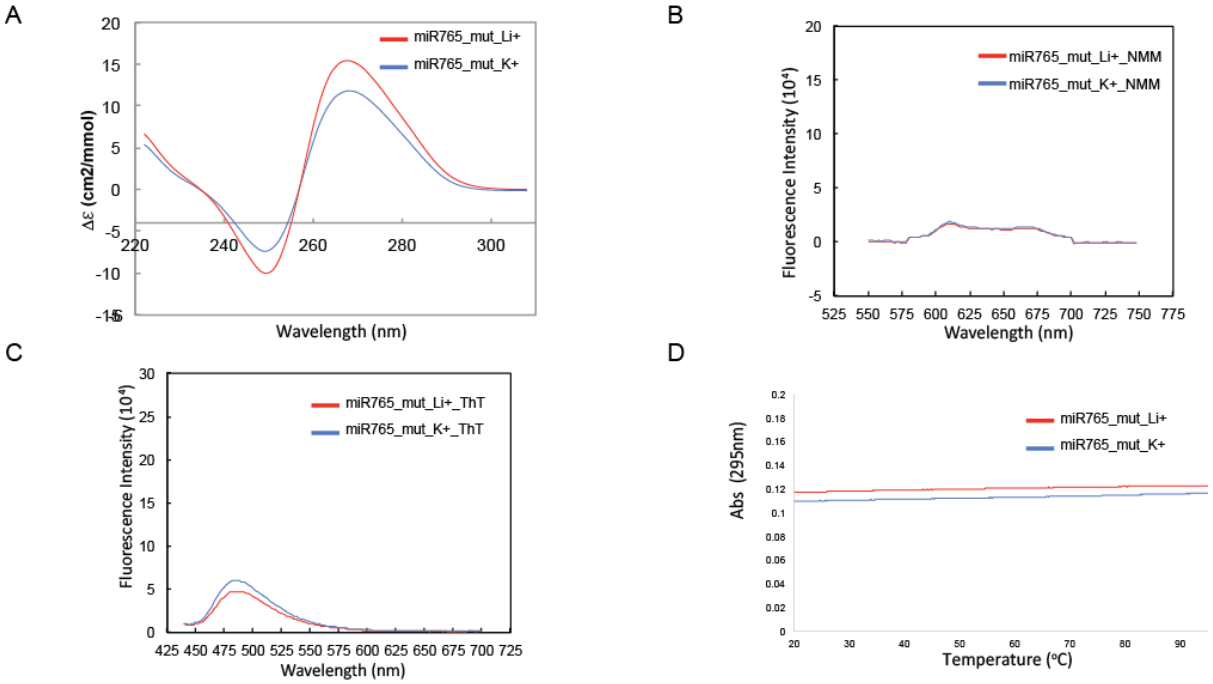

Figure S12. Biophysical characterization of rG4 in miR-765 mutant. A) CD spectrum shows almost no change in the profile under K^+ and Li^+ conditions. **B-C)** Fluorescence spectra show almost identical background fluorescence under K^+ and Li^+ conditions (compare with Fig. 3B-C). **D)** UV melting shows no hypochromic shift at 295 nm. The results of these 4 biophysical assays suggest that no rG4 is formed in the miR-765 mutant.

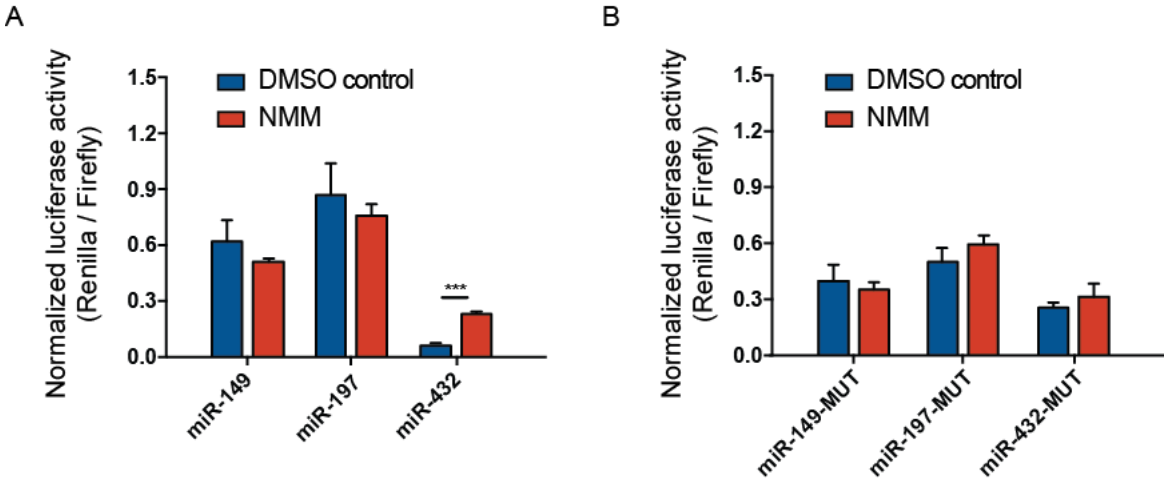

Figure S13. In cell dual luciferase reporter gene assay results and analyses of miR-149, miR-197, and miR-432. Renilla luciferase activity was normalized to Firefly luciferase activity. Average normalized activity of the **A)** wildtype or **B)** mutant reporters 2 days after a co-transfection with wildtype or mutant miRNA mimics relative to that with the scrambled miRNA mimics (negative control), normalized to the firefly luciferase activity. The cells were treated with 80 μM NMM or DMSO for 2 days after the transfection. Normalized luciferase activity was presented as means ± SEM of 3 transfection replicates. Statistical significance was analyzed using Student's two-tail t-test. ***$p<0.001$, relative to DMSO controls.

References

1. A. Kozomara and S. Griffiths-Jones, *Nucleic Acids Res.*, 2014, **42**, D68-73.
2. J. L. Huppert and S. Balasubramanian, *Nucleic Acids Res.*, 2005, **33**, 2908-2916.
3. J. M. Garant, J. P. Perreault and M. S. Scott, *Bioinformatics*, 2017, **33**, 3532-3537.
4. A. Bedrat, L. Lacroix and J. L. Mergny, *Nucleic Acids Res.*, 2016, **44**, 1746-1759.
5. A. B. Sahakyan, V. S. Chambers, G. Marsico, T. Santner, M. Di Antonio and S. Balasubramanian, *Sci Rep*, 2017, **7**, 14535.
6. C. K. Kwok, Y. Ding, S. Shahid, S. M. Assmann and P. C. Bevilacqua, *Biochem J*, 2015, **467**, 91-102.
7. C. K. Kwok, A. B. Sahakyan and S. Balasubramanian, *Angew. Chem. Int. Ed.*, 2016, **55**, 8958-8961.
8. V. T. Mukundan and A. T. Phan, *J. Am. Chem. Soc.*, 2013, **135**, 5017-5028.
9. C. K. Kwok, G. Marsico, A. B. Sahakyan, V. S. Chambers and S. Balasubramanian, *Nat. Methods*, 2016, **13**, 841-844.
10. B. Kankia, D. Gvarjaladze, A. Rabe, L. Lomidze, N. Metreveli and K. Musier-Forsyth, *Biophys. J.*, 2016, **110**, 2169-2175.
11. E. Hatzakis, K. Okamoto and D. Yang, *Biochemistry*, 2010, **49**, 9152-9160.
12. J. L. Mergny, A. T. Phan and L. Lacroix, *FEBS Lett.*, 1998, **435**, 74-78.